

# High purity fructose from inulin with heterogeneous catalysis – from batch to continuous operation

*(Running title) Continuous hydrolysis of inulin*

Andrea Pérez Nebreda<sup>a\*</sup>, Vincenzo Russo<sup>b</sup>, Martino Di Serio<sup>b</sup>, Kari Eränen<sup>a</sup>, Dmitry Murzin<sup>a</sup>, Tapio Salmi<sup>a</sup>, Henrik Grénman<sup>a,c\*</sup>

<sup>a</sup>Åbo Akademi University, Johan Gadolin Process Chemistry Centre, Laboratory of Industrial Chemistry and Reaction Engineering, FI-20500 Turku/Åbo, Finland

<sup>b</sup>University of Naples “Federico II”, Chemical Sciences Department, Via Cintia 4, IT-80126 Naples, Italy

<sup>c</sup>Åbo Akademi University, Molecular Process and Materials Technology, FI-20500 Turku/Åbo, Finland

\*Email: [henrik.grenman@abo.fi](mailto:henrik.grenman@abo.fi)

## Acknowledgements

This work is a part of the activities of the Johan Gadolin Process Chemistry Centre, a center of excellence financed by Åbo Akademi University. Financial support from the Academy of Finland (T. Salmi) and Raison Tutkimussäätiö (A. Pérez Nebreda) is gratefully acknowledged.

## Abstract

**BACKGROUND:** Inulin is a valuable source of high purity fructose. The conversion of inulin to fructose utilizing an advanced sulfonic ion-exchange resin was previously investigated in detail in a batch reactor study, where a detailed mechanistic model for the reaction kinetics was demonstrated (*J Chem Technol Biotechnol* 2018;93:224-232). The same catalyst was employed in tailor made continuous fixed-bed reactors in the current work in order to study the feasibility of continuous operation.

**RESULTS:** Two types of reactors were utilized: a single-bed reactor and a multi-bed reactor with sample withdrawal between catalyst beds. The results from the single-bed reactor allowed finding optimal reaction conditions which were extrapolated and used for the experiments in the multiple-bed reactor. High yields of fructose (75%) were obtained with the multiple-bed reactor without any degradation products. Detailed flow characterization was performed on the reactor system and residence time distribution results were merged with the detailed model for the chemical kinetics obtained from batch reactor studies taking into

account mass transfer limitations, in order to obtain a rigorous model for the performance of the continuous reactor. The fit of the mathematical model to the experimental data was very good and this provides a useful tool for further development and scale-up purposes.

**CONCLUSIONS:** The results of the two related studies highlight the potential of new reactor design strategies towards the realization of more efficient, sustainable and green processes, which can easily be scaled-up and implemented in bio-based industry.

**Keywords:** Heterogeneous Catalysis, Kinetics, Mathematical Modelling, Process Development, Mass Transfer

## Highlights

- A novel multi-bed reactor was used for hydrolysis of inulin
- Intermediate sampling allowed tracking progress of the reaction along the reactor
- High yields of fructose production were obtained
- The process was modelled by considering chemical kinetics and residence time distribution

## 1. Introduction

Fructose is widely used in alimentary industry due to its unique sweetness and its physical and functional properties. It is considered the sweetest sugar found in nature and when it is added to food and drinks it enhances flavor, color, palatability and product stability (1,2).

Fructose has also numerous uses in non-food applications, for instance, it can be utilized as a feedstock to produce bulk chemicals, such as ethanol, acetone-butanol or 2,3-butanediol (3). Moreover, fructose is the main feedstock for producing furan, which is used to synthesize a large variety of specialty chemicals. Dehydration of fructose in acidic media yields hydroxymethylfurfural (HMF), a starting material for many interesting applications, such as

furanic oligomers, cyclomers and polymers. HMF can also react further to produce levulinic acid, an important platform chemical (4,5).

The current processes for commercial fructose production are often based on enzymatic isomerization of glucose, obtained from hydrolysis of corn starch. The enzymatic process is suboptimal as it produces an equimolar mixture of fructose and glucose, from which fructose has to be separated. Costly separation and refining processes, such as chromatographic separation, are needed to obtain high fructose corn syrup (HFCS) (6–8). Direct hydrolysis of fructose-containing polysaccharides, such as inulin, is a promising alternative to enzymatic processes for producing high purity fructose (9).

Inulin is a heteropolysaccharide, present in many fruits and vegetables as an energy storage carbohydrate. It is very abundant in chicory root (*Cichorium intybus*), which is the non-edible part of the chicory plant. Chicory root is most commonly used in industrial scale for the production of inulin (10), which consists of a linear chain of  $\beta$ -2,1-fructose units, commonly having a glucose unit as the chain terminating group. It has a degree of polymerization ( $DP$ ) ranging from 4 to 60, with average  $DP_{av} = 12$  (11). Fructose can be obtained from inulin by either enzymatic or acid hydrolysis. Acid hydrolysis can be carried out with mineral acids (e.g. hydrochloric acid or sulfuric acid) (12) or heterogeneous acid catalysts (13,14) which act on the substrate by breaking down the glycosidic linkage of the inulin chain. Also zeolites (15) and ionic liquids have been demonstrated to successfully hydrolyze inulin (16,17).

The aim of the present work was to demonstrate the feasibility of the hydrolysis of polysaccharides in a continuous reactor by obtaining high yield of sugars and avoiding degradation products. Inulin was chosen as a model compound since it has a relatively simple structure but it still represents polysaccharides well. A continuous packed bed reactor offers many advantages compared to homogeneous batch systems: no need for further separation, continuous operation, low corrosion and efficient temperature control. The catalyst of choice was a commercial ion-exchange resin, which has performed well in previous batch studies with polysaccharides (18–20). It has a relatively high thermal stability and possesses very high acidity for catalyzing the reaction. Conventional porous catalysts

suffer typically from internal mass transfer limitations with large substrate molecules such as inulin, however, all the active acid groups of Smopex-101 are concentrated on the outer surface of the catalyst increasing availability and the efficiency of the catalyst. The back bone of Smopex-101 is a styrene-grafted polyolefin fiber. Hydrolysis of inulin with Smopex-101 was demonstrated to be efficient in a batch reactor in a recent study by our group (21). Two different reactor configurations were used to investigate the hydrolysis of inulin in continuous process, study the flow characteristics in the beds and develop the reactor configuration. A single catalyst bed reactor was used for preliminary experiments aimed at quantifying bed performance and flow characteristics. Based on the preliminary results, a reactor consisting of 5 catalyst beds and intermediate sampling valves was constructed and used to evaluate and demonstrate the reactor performance.

The current work is direct continuation of a previous study performed with the same catalyst in a batch reactor. (21) In that study, the chemical kinetics of inulin hydrolysis were in detail studied, the catalyst performance was evaluated and a detailed mechanistic model was developed for describing the hydrolysis kinetics. In the current work, the detailed model for the chemical kinetics was utilized in the overall model describing the performance of the continuous reactor, which takes also into account the residence time distribution and mass transfer limitations. Overall, the results obtained in the current work demonstrate the feasibility of the process and combining the results of the two studies and merging them in the modeling provides a very strong basis for further process development.

## **Materials and methods**

### **1.1. Materials**

Inulin from chicory (Sigma Aldrich) with an average degree of polymerization of 36 was used as the substrate in the experiments. Inulin is provided as a white powder and it has a fructose-to-glucose ratio of 20:1. Commercial inulin powder can include variable amounts of water which affects the purity of the substrate, thus volumetric Karl Fisher (KF) titration (22)

was utilized to determine the water content. A specific method developed by Ronkart et al. (23) for determining the water content in inulin powder was used. The total content of water in the inulin powder was determined to be 7 wt-%.

Smopex-101 (Johnson Matthey) was used as the catalyst in the packed bed reactors. Smopex-101 is a non-porous styrene sulfonic acid grafted polyolefin fiber with a mean particle diameter of 40  $\mu\text{m}$  and an average fiber length of 250  $\mu\text{m}$ . The cation exchange capacity was 3.6  $\text{mmol}_{\text{eq}}/\text{g}$  on a dry basis (24,25).

## 1.2. Reactor setup

Two different setups were used in the experiments. First, a double jacketed single bed glass reactor (Figure 1A) was used to conduct preliminary experiments. The dimensions are displayed in Table 1. The external jacket of the reactor was connected to a thermostatic bath (Grant Scientific TX150) with water as the heating medium, enabling precise temperature control. The inulin solution was fed into the system by a HPLC pump (Knauer Azura P2.1S) which provided a high precision flow rate. Samples were obtained from a three-way valve located at the reactor outlet. The catalyst was packed inside the reactor in a single bed and glass beads and quartz wool were used as inert packings for the remaining reactor volume.

Based on the preliminary results with the single catalyst bed, a larger double jacketed glass reactor encompassing five successive catalyst beds (Figure 1B), with intermediary sampling provided by valves, was constructed. Each catalyst bed contained 2.5 g of catalyst and the local pH inside each bed was 0.136. Local pH was calculated taking into account the volume occupied by the bed, the mass of the catalyst and the acidity of the catalyst. The catalyst beds were packed with the same technique as the single-bed reactor: glass beads and quartz wool were used as supporting material between the beds. The bed void fraction ( $\epsilon_v$ ) was determined experimentally. A three-way valve was located at the reactor outlet allowing

sampling after the last bed. Inulin was fed into the reactor with the precision HPLC pump, as previously described.

### **1.3. Experimental procedure**

The experiments were conducted using the same procedure with both reactors. The inulin solution was prepared by dissolving a predetermined amount of inulin powder into distilled water applying heating and mixing, until it was completely dissolved. The solution was placed in the feed bottle and connected to the HPLC pump with a polypropylene tube equipped with a Teflon filter. The water bath was turned on and allowed to reach the desired reaction temperature and the experiment was initiated by turning on the pump. The samples from the single bed reactor were taken from the outlet valve and collected in HPLC vials, while for the multibed reactor, the samples were collected after each bed with the help of a syringe equipped with a long needle. Samples were collected at different times-on-stream. The experimental matrix including temperature, flow rate, amount of catalyst, and the initial concentration of inulin can be seen in Table 2. The experimental planning was based on results obtained from batch reactor experiments (21).

### **1.4. Analysis**

The concentrations of fructose, glucose and inulin in the samples were determined by high-pressure liquid chromatography (HPLC), after proper calibration. The column was an Aminex® HPX-87C, 300 mm x 7.8 mm, which is optimized for analyzing monosaccharides, but it also provides class separation of some oligomers. It is primarily used for the quantification of glucose and fructose in HFCS and general monosaccharide analysis. The column was operated with a VWR Hitachi Chromaster, with 5450 RI detector, 5310 column oven, 5210 autosampler and 5110 pump. A 30-min method was used at a temperature of

85°C and the flow rate for the carrier solution (1.2 mM CaSO<sub>4</sub>) was 0.5 mL/min. The samples did not require any pretreatment for this analysis.

The peak separation for the three components was very good. However, it has been observed that small amounts of sulfonic groups can be leached from Smopex-101, especially in the initial stages of the experiment, which are detected at the same retention time as inulin in the HPLC analysis. To avoid this, the reactor was flushed with distilled water until no sulfonic groups could be detected. The amount of sulfonic groups leached in the flushing was so minor, that it did not influence the catalyst performance even though it was visible in the analysis, as has been shown in a previous study.(21)

## **2. Results and discussion**

### **2.1. Single bed reactor**

Preliminary experiments were carried out with the single bed reactor at two different temperatures and flow rates. The obtained average concentrations for inulin, glucose and fructose can be seen in Figure 2 along with the yields of fructose for each of the experiments. Steady state was successfully achieved in all the experiments. As revealed by Figure 2, the yields of monomers increased very logically when decreasing the flow rate, i.e. applying a longer residence time. An increase in the reaction temperature lead to higher fructose concentrations, as the hydrolysis kinetics is strongly influenced by temperature. Presence of intermediate oligomers was not noticed in the experiments. This may be due to the low conversions achieved, as the hydrolysis of inulin follows an end-biting mechanism (21) and the first monomeric units detached from the molecule are located in the ends. Oligomers with high DP are still closer to the structure of unreacted inulin.

Moreover, preliminary results of the flow characteristics were obtained under dynamic conditions before reaching steady state.

## 2.2. Multi-bed reactor

A number of hydrolysis experiments were carried out with the multibed reactor to study its performance. The main advantage of this reactor is that it is possible to monitor the concentration of the reactants along the axial coordinate of the reactor with this configuration, which enables detailed kinetic studies. The temperature in all the experiments was set to 95°C, which was practically the highest obtainable temperature, as the reactor was operated at ambient pressure.

Three different flowrates were used, ranging from a rather high flow to the lowest flow that the pump could provide, avoiding pressure drop issues. The hydrolysis yield at the different flow rates is depicted in Figure 3. Comparison with the single bed reactor can be made from the results; at the same conditions (95°C and 0.5 mL/min) at the end of the first bed with the same amount of catalyst, the same yield value was obtained (36%). Steady state was achieved in all the experiments, as the concentrations obtained after each bed were the same after different times-on-stream. For the highest flow-rate (5 mL/min), the results show a steady performance, but low yield (31.5%). When the flow rate was decreased, a higher yield was achieved, as can be seen in Figure 3. The yield at the reactor outlet for the experiment carried out at 1.25 mL/min was 71%. Reducing the flowrate to 0.5 mL/min did not result in a much higher yield to monomers (74%).

The results displayed in Figure 4 show that not all the inulin reacted directly to monomers, but intermediate products (mainly dimers) were obtained. This complies with the observations made in the batch reactor experiments performed with the same catalyst, where the oligomer concentrations were studied in detail as a function of reaction time utilizing gas chromatography.<sup>(21)</sup> It was concluded that, in practice, the concentrations of compounds with DP exceeding 3 were negligible, with dimers being the most significant fraction among the intermediate products. The results can be rationalized by considering

hydrolysis to proceed, partly via a consecutive reaction pathway where short oligomers are the intermediate species, and partly as inulin direct conversion to monomers. However, the dimers appear to be the most stable intermediates. The bonds located at the ends of the molecule are more likely to meet the reactive protons, resulting in the excision of terminating the sugar units. This mechanism of 'end-biting' hydrolysis allows the molecule to progressively reduce its size directly to more monomers, rather than to oligomers with high DP.

The presence of dimers is more noticeably when the residence time was increased, as can be seen from Figure 4. This may indicate that there are strong mass transfer limitations, as increasing the reaction time did not lead to full conversion. However, presence of degradation products was not observed even at high residence times meaning that the conditions are far from being too harsh to degrade the monomers, mainly fructose, as it is more sensitive to thermal degradation.

### **2.3. Residence time distribution and axial dispersion coefficient determination**

Several step and pulse experiments were carried out in the multibed reactor to study the fluid dynamics of the reactor and to determine the residence time distribution (RTD). The experimental matrix is displayed in Table 3.

The step experiments were performed by using inulin as a tracer. The concentration at the inlet was changed abruptly from 0 to  $C_{0,inu}=5\text{g/L}$  at  $t=0$  and kept constant. The response was measured at the outlet as the concentration of the tracer. Inulin was chosen as the tracer, as it represents best the reaction mixture. The hydrolysis reaction is strongly influenced by temperature and below  $60^\circ\text{C}$  the hydrolysis reaction is very slow and at ambient temperature no reaction can be observed, i.e. inulin acts as an inert tracer. However, the hydrolysis

reaction is performed at a higher temperature ( $>90^{\circ}\text{C}$ ) at which the physical properties of the fluid, namely density and viscosity, are different and the degree of polymerization of the inulin decreases as the reaction progresses along the reactor. To evaluate the RTD in the most similar conditions to the experiments, RTD experiments were also conducted at the reaction temperature ( $95^{\circ}\text{C}$ ). The outlet concentration was measured as a sum of fructose, glucose and inulin concentrations.

The pulse experiments were carried out by injecting a small volume of a high concentration solution of inulin ( $C_{0,inu}=50\text{g/L}$ ) at  $t=0$  in a short period of time. The concentration of the products' sum at the outlet was measured as a function of time.

The results from the RTD experiments were used to determine the axial dispersion coefficient and thus, obtain the Péclet number. The axial dispersion model is often used to describe the behavior in tubular reactors and it characterizes the mass transfer and turbulence in the longitudinal direction with an axial dispersion ( $D_z$ ). The axial dispersion parameter accounts for both molecular diffusion and convection mechanisms.  $D_z$  gives an idea of the performance of the reactor, e.g. when  $D_z=0$ , it means that the reactor is a plug flow and when  $D_z \rightarrow +\infty$ , the reactor behaves as a continuous stirred tank reactor. The mass balance can be written as

$$\frac{\partial C_{inu}}{\partial t} = -u \frac{\partial C_{inu}}{\partial z} + D_z \frac{\partial^2 C_{inu}}{\partial z^2} \quad (1)$$

The following boundary conditions for a closed system were applied:

$$C_{inu}|_{z=0} = \begin{cases} 0 \leq t \leq t_{inj}, & C_{inu} = C_{inu,0} \\ t > t_{inj}, & C_{inu} = 0 \end{cases} \quad (2a)$$

$$C_{inu}|_{z=0} = C_{inu,0} \quad (2b)$$

$$\left. \frac{\partial C_{inu}}{\partial z} \right|_{z=L} = 0 \quad (3)$$

As the initial condition, an 'empty' reactor was considered, i.e.  $C_{inu}=0$ ,  $t=0$ ,  $0 \leq z \leq L$ .

Eq. 2a is valid for a pulse experiment, while Eq. 2b for a stepwise.

For the pulse experiment,  $t_{inj}=V_{loop}/Q$ ; where  $t_{inj}$  is the short time at which the injection took place and  $V_{loop}$  is the small volume of solution injected, for the case of step change.

Depending on the experiment, two analytical solution of the mass balance with axial dispersion for a closed system can be written (26,27):

$$F(t) = \frac{1}{2} \left[ 1 - \operatorname{erf} \left( \frac{L-ut}{\sqrt{4D_z t}} \right) \right] \quad (4)$$

$$E(t) = \frac{u}{\sqrt{4\pi D_z t}} \exp \left[ -\frac{(L-ut)^2}{4D_z t} \right] \quad (5)$$

where  $F(t)$  is the cumulative residence-time distribution curve, calculated by dividing the outlet concentration values by the inlet concentration of the tracer, used in this paper to elaborate the stepwise experiments, while  $E(t)$  is the residence time distribution function used to interpret the pulse experiments. Figure 5 represents the experimental data obtained at 5mL/min paired with the solution of the equations 4 and 5, for both step and pulse experiments. It can be seen that the results are properly described by the equations, since the fit to the curve is very well done. The axial dispersion coefficient is obtained from these results and represent well the system described.

The bed void fraction ( $\epsilon_v$ ) was determined experimentally. The packed column was weighted with the catalyst bed and packing support dry and then filled completely with water and weighted again. The difference gave the void content and void fraction was calculated by dividing by the volume of the empty column in the absence of packing. The result was  $\epsilon_v=0.30$ , which is in accordance with the average value (0.31) calculated from all the RTD results. The Péclet number ( $Pe=uL/D_z$ ) was calculated from the solution of the equation (4) for each RTD experiment. The results for the  $Pe$  number for each of the experiments can be seen in Table 3. An average value of  $Pe$  for all the experiments was found to be 113. The results of  $Pe$  as a function of flowrate and temperature can be seen in Figure 6. The reciprocal of Peclet number is the degree of dispersion (26). For this case, it is approx. 0.01, which in this case indicates in physical terms that the shape of the axial concentration profile

changes considerably in the time interval for the liquid to flow through the reactor. Axial dispersion cannot be completely neglected in any case. It can be observed that the values of Pe number are quite similar for all the tested conditions, proving that the temperature does not significantly influence the dispersion mechanism. For the higher flowrate experiments, the Pe number decreases slightly meaning that the convection mechanism is more predominant than the mass transfer.

## 2.4. Reactor modelling

A dynamic external diffusion model was selected to describe the behavior of the multibed tubular reactor. The model is composed by coupling two mass balance equations: (i) liquid bulk mass balance, where convection, axial dispersion and liquid-solid mass transfer are considered; (ii) solid surface mass balance, where the reaction is considered equal to the liquid-solid flux at steady-state condition.

The mass balance of inulin in the liquid bulk is

$$\frac{\partial C_{inu}}{\partial t} = -u \frac{\partial C_{inu}}{\partial z} + D_z \frac{\partial^2 C_{inu}}{\partial z^2} - k_s a_{sp} (C_{inu} - C_{inu,S}) \quad (6)$$

where superficial velocity can be described as

$$u = \frac{Q}{A \cdot \varepsilon_v} \quad (7)$$

The pseudo steady-state condition at the catalyst surface

$$k_s a_{sp} (C_{inu} - C_{inu,S}) + v_{inu} r = 0 \quad (8)$$

where  $k_s$  is the mass transfer coefficient in the liquid film surrounding the catalyst particle and  $a_{sp}$  is the catalyst surface area per reactor volume ( $a_{sp}=4.73 \cdot 10^4 \text{ m}^2/\text{m}^3$ ). The mass transfer coefficient  $k_s$  was estimated with Coeuret's correlation (28):

$$Sh_p = 5.4 Re_p^{1/3} Sc^{1/4} \quad (9)$$

which is valid for  $0.04 < Re_p < 30$  and  $1700 < Sc < 11000$ . Eq 9. is an empirical correlation for the mass transfer coefficient determination for a fixed bed of particles with a liquid flowing at low Reynolds numbers. The dimensionless groups are defined as

$$Sh_p = \frac{k_s d_p}{D} \quad (10)$$

$$Re_p = \frac{u d_p}{\nu} \quad (11)$$

$$Sc = \frac{\nu}{D} \quad (12)$$

The kinematic viscosity (29) was considered temperature dependent as in Eq. 13, while the particle diameter was calculated as equivalent diameter value, leading to  $d_p = 9.96 \cdot 10^{-5} \text{m}$ .

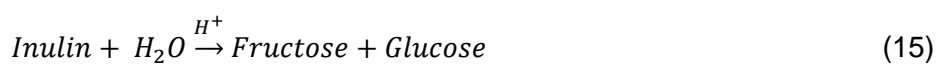
$$\nu [m^2 / s] = 1.814 \cdot 10^{-2} \exp\left(-\frac{T[K]}{29.05}\right) + 2.687 \cdot 10^{-7} \quad (13)$$

The diffusivity of the substrate in water changes with the conversion ( $X_m$ ) degree, because as the reaction proceeds, the molar volume of the substrate changes accordingly. Thus, the molar volume of the reactant was updated with the equation,

$$V_{m, inu} = [X_m + DP(1 - X_m)]V_{m, fru} \quad (14)$$

Where  $V_{m, inu}$  is the molecular volume for inulin that changes with the conversion degree and  $V_{m, fru}$  is the molecular volume for fructose and it is  $111 \text{ cm}^3/\text{mol}$ . (30) Equation 14 was inserted in the Wilke-Chang equation for determination of the diffusion coefficient of the reaction mixture in the aqueous solution. (31,32)

The kinetic modelling for the hydrolysis of inulin in the presence of a heterogeneous catalyst was well described in our previous work (21). The reaction rate was observed to be slow in the beginning of the reaction but it increased rapidly as the reaction progresses. The  $DP$  of the inulin molecule decreases along the reaction, because the protons from the catalyst break the glycosidic bonds. The overall reaction is described as



The glucose-to-fructose ratio is so small that the obtained glucose concentration is almost negligible, so for the sake of simplicity a lumped product is considered, e.g. the sum of fructose and glucose expressed as monomers. The reaction rate expression is presented as follows,

$$r = kC_{H^+}C_{inu,S}(1 + \beta X_m^\alpha) \quad (16)$$

The model presented describes the hydrolysis reaction with two autocatalysis parameters,  $\alpha$  and  $\beta$ , which were used to describe the accelerating kinetics in the model. The values obtained after parameter estimation were  $\alpha=0.89$  and  $\beta=4.14$  (21). The parameter  $\alpha$  is the exponent which influences how the rate constant changes with conversion and  $\beta$  indicates the presence of autocatalysis and its influence on the reaction rate. The conversion of inulin is described by the following equation,

$$X_m = 1 - \frac{C_{inu,S}}{C_{inu,0}} \quad (17)$$

Eq. (17) neglects the formation of oligomers.

The model was implemented in gPROMS Model Builder v.4.0 software (33), discretizing the axial coordinates with the implemented method of lines, by using the backward finite difference method with 100 discretization elements. (34,35)

In Figure 7, the results can be seen for the three different flow rates as a function of the inulin conversion and dimensionless length when the Coeuret correlation is applied. The  $R^2$  value describing the fit of the model to experimental data obtained the value 0.91.

The estimation of the external mass transfer effect is correct, since the model describes well the results obtained. The presence of mass transfer limitations affects to the performance of the reactor, explaining why the achieved conversion is limited.

The correlation applied as it is may not represent well the mass transfer phenomena at low  $Re$ , as in the determination of the correlation by Coeuret et al. (28), the scattering of the data was evident.

For this reason, a parameter estimation was done with the intention of obtaining a better description of the experimental data. The results are reported in Figure 8.

As can be seen, the model is able to better describe the experimental data. The  $R^2$  value describing the fit of the model to experimental data obtained the value 0.95 compared to the value 0.91 obtained when employing the Coeuret correlation. In this case a  $k_s=5.0 \cdot 10^{-8} \pm 1.1 \cdot 10^{-8}$  m/s that is roughly between two and three orders of magnitude lower than the one obtained strictly by using the Coeuret correlation. This effect can be justified as Coeuret found that the highest uncertainties on the correlation predictions were observed for  $Re_p$  lower than 0.1 (in our case roughly 0.05), finding that the experimental points can be scattered of 2-3 orders of magnitude.

## Conclusions

The results presented in the current work show that the hydrolysis of inulin to fructose is feasible in a continuous packed bed column reactor containing a fibrous heterogeneous catalyst. The results show that operating at optimal temperature and flowrate leads to high concentrations of fructose in the outlet and no degradation products are observed. Only minor amounts of unreacted oligomers are present in the final mixture. A multiple packed bed was investigated, in which intermediate sampling between the catalytic beds was performed to determine the progress of the reaction along the reactor. This configuration was useful to follow the kinetics and mass transfer phenomena influencing the reactor performance.

A fluid-dynamic characterization was performed by conducting several residence time distribution experiments, both pulse and step experiments. Mathematical modelling was utilized to interpret the collected data. The results showed a good agreement with the proposed model and the determined values for the axial dispersion coefficient indicated low axial

dispersion, roughly invariant with both temperature and fluid velocity in the investigated range of operational conditions.

The inulin hydrolysis experiments conducted in the multiple packed bed reactor were simulated by solving the mass balance equations governing the system, taking into account both the axial dispersion and the mass transfer limitations in the liquid film surrounding the catalyst particles. Couret's correlation developed for packed bed reactors was applied; molar volumes were considered to be dependent on the polymerization degree, as the molecules diminish in size when the reaction proceeds. The experimental data trend was correctly simulated, but a deviation between the data and the model prediction was evident. For this reason, the mass transfer coefficient was estimated based on the experimental data. The obtained optimal parameter value was determined to fall in the window of error of the Couret's correlation at Reynolds particle numbers lower than 0.1.

The results obtained in the present work contribute significantly to the scale-up of the hydrolysis of inulin in a continuous reactor utilizing a heterogeneous catalyst.

## References

1. Position of the american dietetic association: Use of nutritive and nonnutritive sweeteners. *J Am Diet Assoc.* 2004;104(2):255–75.
2. White JS. Sucrose , HFCS , and Fructose : History , Manufacture , Composition , Applications , and Production. In: Springer, editor. *Fructose, High Fructose Corn Syrup, Sucrose and Health.* Humana Press; 2014. p. 13–33.
3. Jones DT, Woods DR. Acetone-butanol fermentation revisited. *Microbiol Rev.* 1986;50(4):484–524.
4. Bozell JJ, Moens L, Elliott DC, Wang Y, Neuenschwander GG, Fitzpatrick SW, et al. Production of levulinic acid and use as a platform chemical for derived products. *Resour Conserv Recycl.* 2000;28(3–4):227–39.

5. Rosatella A a., Simeonov SP, Frade RFM, Afonso C a. M. 5-Hydroxymethylfurfural (HMF) as a building block platform: Biological properties, synthesis and synthetic applications. *Green Chem.* 2011;13(4):754.
6. Lima DM, Fernandes P, Nascimento DS, Figueiredo Ribeiro RDC, de Assis SA. Fructose syrup: A biotechnology asset. *Food Technol Biotechnol.* 2011;49(4):424–34.
7. Mark L, White S. Manufacturing, composition, and applications of fructose. *Am J Clin Nutr.* 1993;58(suppl):724–32.
8. Subramani HJ, Hidajat K, Ray a. K. Optimization of Simulated Moving Bed and Varicol Processes for Glucose–Fructose Separation. *Chem Eng Res Des.* 2003;81:549–67.
9. Fuchs A. Potentials for Non-Food utilization of Fructose and Inulin. *Starch/Stärke.* 1987;39(10):335–43.
10. Bosscher D. Fructan Prebiotics Derived from Inulin. In: Charalampopoulos D, Rastall RA, editors. *Prebiotics and Probiotics Science and Technology.* New York, NY: Springer New York; 2009. p. 163–205.
11. Roberfroid MB. Introducing inulin-type fructans. *Br J Nutr.* 2005;93(S1):S13.
12. Blecker C, Fougnyes C, Van Herck JC, Chevalier JP, Paquot M. Kinetic study of the acid hydrolysis of various oligofructose samples. *J Agric Food Chem.* 2002;50(6):1602–7.
13. S.H. Khan KR. Inversion of sucrose solution by ion exchange: evaluation of reaction rate and diffusivity. *Chem Eng J.* 1996;61(1):7–12.
14. H. Yamazaki KM. Production of fructose syrup. U.S. Patent; 4,613,377, 1986.
15. Abasaeed a. E, Lee YY. Inulin hydrolysis to fructose by a novel catalyst. *Chem Eng Technol.* 1995;18(6):440–4.

16. Zhao Z, Wang X, Zhou G, Cao Y, Lu P, Liu W. Hydrolysis kinetics of inulin by imidazole-based acidic ionic liquid in aqueous media and bioethanol fermentation. *Chem Eng Sci.* 2016;151:16–24.
17. Gervasini A, Carniti P, Imparato C, Clayden NJ, Aronne A. *New Nb-Si-P Ternary Oxide Materials and their Use in Heterogeneous Acid Catalysis.* 2017: <http://dx.doi.org/10.1016/j.mcat.2017.10.006>
18. Hilpmann G, Becher N, Pahner F -a., Kusema B, Mäki-Arvela P, Lange R, et al. Acid hydrolysis of xylan. *Catal Today.* 2015;259:376–80.
19. Kusema BT, Tönnov T, Mäki-Arvela P, Salmi T, Willför S, Holmbom B, et al. Acid hydrolysis of O-acetyl-galactoglucomannan. *Catal Sci Technol.* 2012;3:116–22.
20. Kusema BT, Hilpmann G, Mäki-Arvela P, Willför S, Holmbom B, Salmi T, et al. Selective hydrolysis of arabinogalactan into arabinose and galactose over heterogeneous catalysts. *Catal Letters.* 2011;141(3):408–12.
21. Nebreda AP, Salmi T, Murzin DY, Grénman H. High purity fructose from inulin with heterogeneous catalysis – kinetics and modeling. *J Chem Technol Biotechnol.* 2018;93:223-232
22. Margreth M, Bruttel P, Schlink R. *Water Determination By Karl Fischer Titration.* In: *Pharmaceutical Sciences Encyclopedia.* John Wiley & Sons; 2010.
23. Ronkart SN, Paquot M, Fougnyes C, Deroanne C, Van Herck JC, Blecker C. Determination of total water content in inulin using the volumetric Karl Fischer titration. *Talanta.* 2006;70(5):1006–10.
24. Lilja J, Aumo J, Salmi T, Murzin DY, Mäki-arvela P, Sundell M, et al. Kinetics of esterification of propanoic acid with methanol over a fibrous polymer-supported sulphonic acid catalyst. 2002;228:253–67.

25. Nebreda AP, Grénman H, Mäki-Arvela P, Eränen K, Hemming J, Willför S, et al. Acid hydrolysis of O-acetyl-galactoglucomannan in a continuous tube reactor: a new approach to sugar monomer production. *Holzforschung*. 2016;70 (3):187-194.
26. Hill CG, Root TW. Introduction to Chemical Engineering Kinetics & Reactor Design. Second Edi. Vol. 53, *Journal of Chemical Information and Modeling*. Hoboken, New Jersey: John Wiley & Sons; 2013. 1689-1699 p.
27. Levenspiel O. Chemical Reaction Engineering. Third Edit. New York, NY: John Wiley & Sons; 1999. 685 p.
28. Coeuret F. L'electrode poreuse percolante (epp)-I. Transfert de matiere en lit fixe. *Electrochim Acta*. 1976;21(3):185–93.
29. Perry R, Green D, Maloney J. Perry's chemical engineers' handbook [Internet]. *Journal of Chemical Education*. 1997. 2582 p.
30. Kapadnis KH, Hiray AP. Study of Structure Making/Breaking Properties of Glucose, Fructose, Sucrose and Maltose in Aqueous KCl at Various Temperatures. *Chem Sci Trans*. 2013;2(2):485–90.
31. Wilke CR, Chang P. Correlation of Diffusion Coefficients in Dilute. 1955;264–70.
32. Miyabe K, Isogai R. Estimation of molecular diffusivity in liquid phase systems by the Wilke-Chang equation. *J Chromatogr A*. 2011;1218(38):6639–45.
33. gPROMS Model Builder V.3.7.1. Process System Enterprise; 2013.
34. Russo V, Kilpiö T, Martino Di M, Tesser R, Santacesaria E, Murzin DY, et al. Dynamic non-isothermal trickle bed reactor with both internal diffusion and heat conduction : Sugar hydrogenation as a case study. *Chem Eng Res Des*. 2015;102:171–85.
35. Russo V, Kilpiö T, Hernandez Carucci J, Di Serio M, Salmi TO. Modeling of microreactors for ethylene epoxidation and total oxidation. *Chem Eng Sci*.

## Tables

**Table 1.** Reactor dimensions

Type of Reactor	Dimensions		
	Length [cm]	Internal diameter [cm]	Free volume [cm <sup>3</sup> ]
Single bed reactor	40	1.5	70.68
Multiple bed reactor	66	2.5	323.97

**Table 2.** Experimental design

	Experiment	$T$ [°C]	$Q$ [mL <sup>3</sup> /min]	$w_{cat}$ (g)	$C_{0,inu}$ [mg/mL]
Single bed reactor	1	90	1	2.5	5
	2	90	0.5	2.5	5
	3	95	0.5	2.5	5
Multi bed reactor	4	95	5	12.5	5
	5	95	1.25	12.5	5
	6	95	0.5	12.5	5

**Table 3.** Experimental matrix for the RTD experiments

Type experiment	T [°C]	Q [mL/min]	Pe [-]
STEP	95	5	107.79
STEP	20	5	100.99
STEP	20	2.5	123.19
PULSE	20	5	106.76
STEP	95	1.25	124.56
STEP	95	0.5	116.77

Figure legends

**Figure 1.** Schematic representation of: A) single bed reactor; B) multi bed reactor.

**Figure 2.** Average concentrations of inulin, fructose and glucose obtained in the single bed reactor under different experimental conditions. The inulin yields are presented by the single points.

**Figure 3.** Yield to sugar monomers after each catalyst bed at 95°C with different flow rates.

**Figure 4.** Concentration of the different components after each bed at 95°C with different flowrates.

**Figure 5.**  $F(t)$  curve for step and  $E(t)$  curve pulse change experiment at flow rate of 5 mL/min. The points represent the experimental values and the continuous line represents the solution of the equations (4) and (5).

**Figure 6.** Values of  $Pe$  obtained for the different experiments as a function of different flowrates and temperatures.

**Figure 7.** Conversion as a function of dimensionless reactor length. The dots represent the values obtained experimentally and the continuous lines are the results of the simulated experiments with the model applying Coeuret correlation.

**Figure 8.** Conversion as a function of dimensionless reactor length. The dots represent the values obtained experimentally and the continuous lines are the results of the simulated experiments with the model applying parameter estimation.

### **Nomenclature**

$A$  – cross-sectional area [ $\text{m}^2$ ]

$a_{\text{sp}}$  – catalyst surface area [ $\text{m}^2/\text{m}^3$ ]

$C_{0,\text{inu}}$  – Initial concentration inulin [ $\text{mg}/\text{mL}$ ]

$C_{\text{H}^+}$  – Concentration of protons [ $\text{mg}/\text{mL}$ ]

$C_{\text{inu,feed}}$  – Concentration of inulin, feed [ $\text{mg}/\text{mL}$ ]

$C_{\text{inu,S}}$  – Concentration of inulin in the surface of the catalyst [ $\text{mg}/\text{mL}$ ]

$d_p$  – particle diameter [-]

$D$  – Molecular diffusion coefficient [ $\text{m}^2/\text{s}$ ]

$D_z$  – Axial dispersion coefficient [ $\text{m}^2/\text{s}$ ]

$k$  – kinetic constant [ $\text{L}/\text{molmin}$ ]

$k_s$  – mass transfer coefficient [ $\text{m}/\text{s}$ ]

$L$  – length (m)

$Pe$  – Peclet number [-]

$Q$  – flowrate [ $\text{mL}/\text{min}$ ]

$r$  – reaction rate [ ]

$Re$  – Reynolds number [-]

$Sc$  – Schmidt number [-]

$Sh$  – Sherwood number [-]

$T$  – temperature [ $^{\circ}\text{C}$ ]

$t$  – time [s]

$t_{\text{inj}}$  – injection time [s]

$u$  – superficial velocity [ $\text{m}/\text{s}$ ]

$v_{inu}$  – stoichiometric coefficient [-]

$V_{loop}$  – volume injected (mL)

$V_{m,fru}$  – molecular volume fructose [ $\text{cm}^3/\text{mol}$ ]

$V_{m,inu}$  – molecular volume inulin [ $\text{cm}^3/\text{mol}$ ]

$w_{cat}$  – weight catalyst [g]

$X_m$  – conversion [-]

$z$  – length [cm]

$\alpha$  – autocatalysis parameter [-]

$\beta$  – autocatalysis parameter [-]

$\varepsilon_v$  – Void fraction [-]

$\nu$  – kinematic viscosity [ $\text{m}^2/\text{s}$ ]